EPJ Web of Conferences **141**, 01013 (2017)
ISMD 2016
DOI: 10.1051/epjconf/201714101013

Femtoscopy in $\sqrt{s_{\mathrm{NN}}} = 5.02$ TeV p-Pb collisions with *ATLAS*

Michael Clark[1,a] on behalf of the ATLAS Collaboration

[1] *Columbia University, 116th St & Broadway, New York, NY 10027, USA*

Abstract. Bose-Einstein correlations between identified charged pions are measured for p+Pb collisions at $\sqrt{s_{\mathrm{NN}}} = 5.02$ TeV with the ATLAS detector using a total integrated luminosity of 28 nb^{-1}. Pions are identified using ionisation energy loss measured in the pixel detector. Two-particle correlation functions and the extracted source radii are presented as a function of average transverse pair momentum (k_{T}) and rapidity ($y^{\star}_{\pi\pi}$) as well as collision centrality. Pairs are selected with a rapidity $-2 < y^{\star}_{\pi\pi} < 1$ and with an average transverse momentum $0.1 < k_{\mathrm{T}} < 0.8$ GeV. The effect on the two-particle correlation function from jet fragmentation is studied, and a new method for constraining its contributions to the measured correlations is described. The measured source sizes are substantially larger in more central collisions and are observed to decrease with increasing pair k_{T}. A correlation with the local single-particle multiplicity $\mathrm{d}N_{\mathrm{ch}}/\mathrm{d}y^{\star}$ is demonstrated. The scaling of the extracted radii with the mean number of participants is also used to compare a selection of initial-geometry models. The cross term R_{ol}, which couples radial and longitudinal expansion, is measured as a function of rapidity, and a departure from zero is observed with 4.8 σ combined significance for $y^{\star}_{\pi\pi} > -1$ in the most central events.

1 Introduction

Multi-particle correlations in proton-lead (p+Pb) [1–5] and proton-proton ($p + p$) [6] collisions exhibit long-range azimuthal correlations similar to those observed in lead-lead (Pb+Pb) collisions, in which they are attributed to collective expansion of the quark-gluon plasma. Hydrodynamic models can describe the observed correlations in p+Pb [7–9], but the extent to which they are appropriate in "small" systems remains an open question.

Bose-Einstein correlations between charged pion pairs can be used to measure the spacetime extent of particle production with a technique called femtoscopy (see Reference [10] and references therein). The width of the correlations in relative momentum $\mathbf{q}$ is studied as a function of pair transverse momentum k_{T}. The measured Hanbury Brown and Twiss (HBT) radii, which are interpreted as the size of the particle-emitting region at freezeout, are expected to decrease with rising transverse momentum if the source expands [11]. Thus, HBT measurements can be used to address the questions raised by angular correlation results. While femtoscopic methods have already been applied to p+Pb systems at the LHC [12, 13], these results are obtained using a new data-driven technique to constrain the significant background contribution from jet fragmentation, and they provide the first measurements of the dependence of these source radii on the rapidity $y^{\star}_{\pi\pi}$.

---

[a] e-mail: michael.ryan.clark@cern.ch

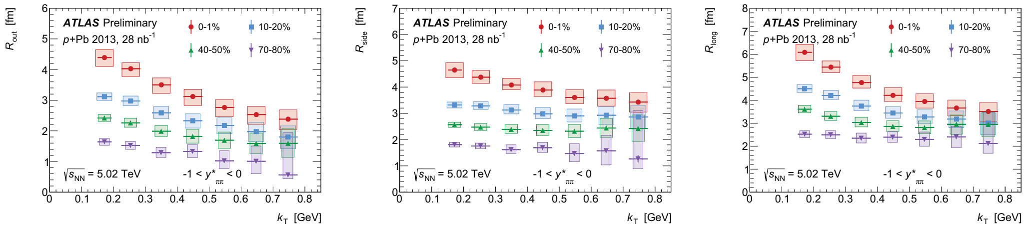

Figure 1. Three-dimensional HBT radii as a function of the average transverse momentum k_{T} of pion pairs [14]. The widths of the boxes vary between centrality intervals only for visual clarity.

2 Experimental Analysis

The data used in this analysis were collected by the ATLAS detector [15] during the 2013 p+Pb run at the Large Hadron Collider (LHC) with a nucleon-nucleon centre-of-momentum energy of $\sqrt{s_{\mathrm{NN}}} =$ 5.02 TeV. The inner detector is used to reconstruct charged particles. It consists of a silicon pixel detector, a semiconductor tracker made of double-sided silicon microstrips, and a transition radiation tracker made of straw tubes. Pions are identified using a measurement of the charge deposited in the pixel detector. All three subdetectors are composed of a barrel and two symmetrically placed end-cap sections. The forward calorimeters, located in a pseudorapidity range of $3.1 < |\eta| < 4.9$, are used to estimate the centrality of each collision.

The two-particle correlation functions are taken to be of the form

$$C_{\mathbf{k}}(\mathbf{q}) = [(1-\lambda) + \lambda K(\mathbf{q}) C_{\mathrm{BE}}(\mathbf{q})]\, \Omega(\mathbf{q})\,, \tag{1}$$

where K is a correction factor for final-state Coulomb interactions and Ω represents non-femtoscopic background which arises due to jet fragmentation. The Bose-Einstein part of the three-dimensional correlation functions are fit to functions of the form

$$C_{\mathrm{BE}}(\mathbf{q}) = 1 + e^{-\|R\mathbf{q}\|}\,, \tag{2}$$

where R is a symmetric matrix in the Bertsch-Pratt coordinate system:

$$R = \begin{pmatrix} R_{\mathrm{out}} & 0 & R_{\mathrm{ol}} \\ 0 & R_{\mathrm{side}} & 0 \\ R_{\mathrm{ol}} & 0 & R_{\mathrm{long}} \end{pmatrix}. \tag{3}$$

In these coordinates, q_{out} is the projection along $\mathbf{k}_{\mathrm{T}}$, q_{side} is the projection along $\hat{\mathbf{z}} \times \mathbf{k}_{\mathrm{T}}$ (with the z-axis along the beamline), and q_{long} is the longitudinal component. The relative momentum of the pair is evaluated in the longitudinally comoving frame (LCMF), i.e., the frame boosted such that $k_z = 0$.

The jet fragmentation background, $\Omega(\mathbf{q})$, contributes an enhancement at low $|\mathbf{q}|$, though usually over a wider range in $|\mathbf{q}|$ and with a smaller amplitude than the Bose-Einstein correlation. This background is constrained in same-charge correlation functions by measuring the opposite-sign correlation functions, which do not contain a Bose-Einstein enhancement. Opposite-charge correlations contain contributions from resonance decays and the most prominent of these are removed by cuts on the opposite-charge pion pair mass. Even with resonances removed, due to charge conservation the fragmentation contribution is not identical between same- and opposite-charge correlations, but the shape

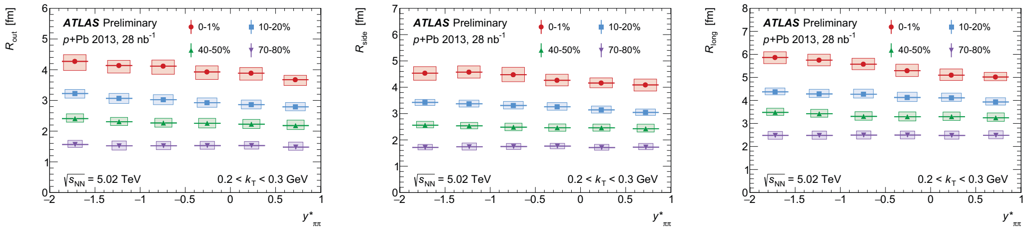

Figure 2. Three-dimensional HBT radii as a function of the rapidity $y^\star_{\pi\pi}$ of pion pairs [14]. The widths of the boxes vary between centrality intervals only for visual clarity.

is similar. The relationship between the two is studied in detail using PYTHIA 8, and a mapping from opposite- to same-charge correlation functions is derived in simulation for use with the data. For details on this and other aspects of the analysis, see Reference [14].

3 Results

Figure 1 shows the HBT radii as a function of k_T in four centrality intervals. A decrease of the radii with rising k_T, interpreted as a signature of collective expansion, is observed in central events. This trend is diminished in peripheral events.

The HBT radii are presented as a function of pair rapidity $y^\star_{\pi\pi}$ in Figure 2. Central collisions exhibit larger radii on the backward (Pb-going) side of the event, while peripheral events show no distinguishable variation of the radii with rapidity.

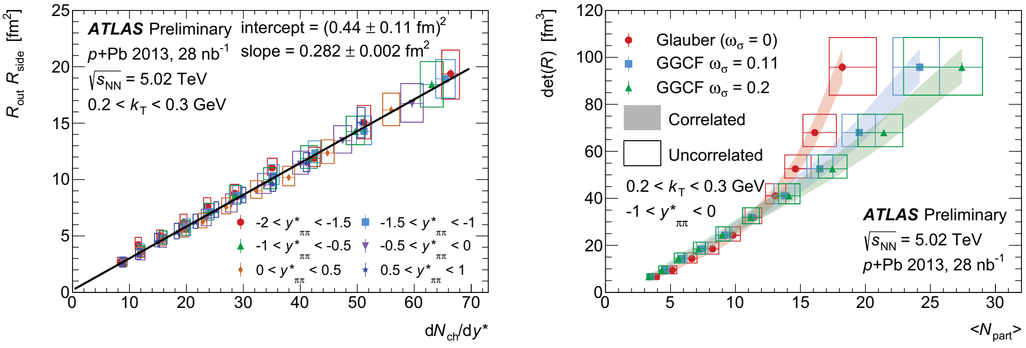

(a) (b)

Figure 3. The transverse area $R_{out}R_{side}$ is shown in (a) as a function of local multiplicity in several intervals of centrality and $y^\star_{\pi\pi}$ [14]. The volume element of the HBT matrix det(R) is shown in (b) as a function of N_{part} for three Glauber-Gribov colour fluctuation models.

Source radii are observed to correlate strongly with the single-particle local multiplicity $dN_{ch}/dy^\star$, as illustrated in Figure 3(a), which presents the transverse area $R_{out}R_{side}$ at $0.2 < k_T < 0.3$ GeV

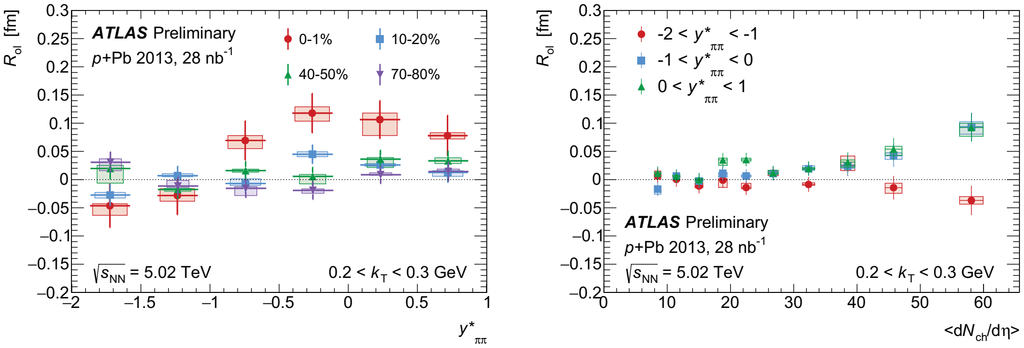

(a) (b)

Figure 4. The cross-term R_{ol}, which couples radial and longitudinal expansion, is shown as a function of rapidity (a) and average global multiplicity $\langle \mathrm{d}N_{\mathrm{ch}}/\mathrm{d}\eta \rangle$ (b) [14].

in several centrality and rapidity intervals as a function of $\mathrm{d}N_{\mathrm{ch}}/\mathrm{d}y^{\star}$. The linear behaviour with multiplicity indicates a constant areal density at low k_{T}.

Figure 3(b) compares the volume scale det(R) with the average number of nucleon participants $\langle N_{\mathrm{part}} \rangle$, both for the standard Glauber model and for two choices of the Glauber-Gribov colour fluctuation (GGCF) extension [16]. This extension of the Glauber initial-geometry model account for fluctuations in the nucleon-nucleon cross section. The volume scale increases at a rate greater than linearly for all choices shown for N_{part}. While the final-state volume indicated by det(R) should not necessarily scale linearly with the initial size N_{part}, extreme departure from a linear behaviour is difficult to describe. These results indicate that fluctuations in the size of the proton are crucial for the understanding of the initial geometry of p+Pb collisions.

The cross-term, R_{ol}, which couples to the lifetime of the source [17], is shown in Figure 4. In hydrodynamic models, a nonzero R_{ol} necessitates both longitudinal and transverse expansion. A significant departure from zero is observed in this parameter in central events, but only for rapidities $y^{\star}_{\pi\pi} \gtrsim -1$. This indicates that the particle production at mid-rapidity and in the proton-going direction is sensitive to the local z-asymmetry of the system.

These results provide a detailed description of the freeze-out geometry of proton-lead collisions. The large pseudorapidity coverage of the ATLAS detector has been utilised to probe the rapidity dependence of the asymmetric p+Pb collisions. Clear signatures of collective behaviour are observed in central collisions, but they are significantly diminished in peripheral collisions.

Acknowledgments

This work was supported by U.S. Department of Energy grant DE-FG02-86ER40281.

References

[1] ALICE Collaboration, Phys. Lett. B **719**, 29 (2013)
[2] ATLAS Collaboration, Phys. Rev. Lett. **110**, 182302 (2013)

[3] CMS Collaboration, Phys. Lett. B **724**, 213 (2013)
[4] ATLAS Collaboration, Phys. Rev. C **90**, 044906 (2014)
[5] CMS Collaboration, Phys. Rev. Lett. **115**, 012301 (2015)
[6] ATLAS Collaboration, Phys. Rev. Lett. **116**, 172301 (2016)
[7] P. Bożek, Phys. Rev. C **85**, 014911 (2012)
[8] E. Shuryak, I. Zahed, Phys. Rev. C **88**, 044915 (2013)
[9] P. Bożek, W. Broniowski, Phys. Rev. C **88**, 014903 (2013)
[10] M.A. Lisa, S. Pratt, R. Soltz, U. Wiedemann, Ann. Rev. Nucl. Part. Sci. **55**, 357 (2005)
[11] P.F. Kolb, U.W. Heinz (2003), `nucl-th/0305084`
[12] ALICE Collaboration, Phys. Rev. C **91**, 034906 (2015)
[13] ALICE Collaboration, Phys. Lett. B **739**, 139 (2014)
[14] ATLAS Collaboration, *ATLAS-CONF-2016-027* (2016), `https://cds.cern.ch/record/2157691`
[15] ATLAS Collaboration, JINST **3**, S08003 (2008)
[16] M. Alvioli, M. Strikman, Phys. Lett. B **722**, 347 (2013)
[17] S. Chapman, P. Scotto, U.W. Heinz, Phys. Rev. Lett. **74**, 4400 (1995)